

Surface elevation and velocity changes on the south-central Greenland ice sheet: 1980–2011

Kenneth C. JEZEK

*Byrd Polar Research Center and Department of Geological Sciences, The Ohio State University, Columbus, OH, USA
E-mail: jezek.1@osu.edu*

ABSTRACT. We extend through 2011 an ice-sheet elevation and surface velocity record across three measurement networks established in south-central Greenland by The Ohio State University in 1980/81. Surface parameters are derived from repeat GPS in situ observations, elevations measured by airborne laser altimetry and by the Ice, Cloud and land Elevation Satellite (ICESat). Elevations at the western network steadily rose early in the record by $0.10 \pm 0.02 \text{ m a}^{-1}$, but an eastward-progressing thinning trend began in the mid-1990s followed by a $\sim 1 \text{ m}$ elevation drop at all stations from 2005 to 2011. Measurements weakly suggest a surface velocity increase at the western cluster from 1980 to 2005. At the central network, elevations rose by $0.08 \pm 0.02 \text{ m a}^{-1}$ through 2005 and surface speed increased by $0.5\text{--}0.7 \text{ m a}^{-1}$. Surface elevations at the central network remained nearly constant thereafter. Thickening occurred at the southern ice divide by $0.05 \pm 0.02 \text{ m a}^{-1}$, while east of the divide the ice sheet thinned with increasing rate from the divide, likely because of decreasing accumulation rate trends and drawdown into rapidly retreating coastal glaciers. Our most recent data show that thinning rates are slowing at several sites just east of the divide and that the elevation at the divide continues to increase.

INTRODUCTION

Satellite altimeter measurements of ice-sheet elevation began in 1975 with the launch of Geostationary Operational Environmental Satellite-3 (GOES-3; Brooks and others, 1978). Data from follow-on sensors establish an important record of elevation change that reveals complex spatial and temporal variations in surface elevation. Zwally and others (1989) analyzed GOES-3, Seasat and Geosat (1975–86) altimeter data and found that the southern half of Greenland was thickening by $\sim 0.20 \pm 0.06 \text{ m a}^{-1}$, with a possible increase in thickening rate to $0.28 \pm 0.02 \text{ m a}^{-1}$ for the later part of the record. However, Davis and others (2000) using reprocessed Seasat and Geosat (1978–88) concluded that southern Greenland ice-sheet elevations were essentially constant on average, though smaller sectors particularly relevant to this paper show thickening rates of up to 0.15 m a^{-1} . Johannessen and others (2005) analyzed 1992–2003 data from the two European Remote-sensing Satellites (ERS-1/-2) to show that ice thickness increased on average by $0.064 \pm 0.2 \text{ m a}^{-1}$ at elevations above 1500 m. Below 1500 m, they found a thinning rate of $0.02 \pm 0.009 \text{ m a}^{-1}$. In a recent paper, Zwally and others (2011) compared Ice, Cloud and land Elevation Satellite (ICESat) data (2003–07) with ERS and airborne data (1992–2002). They found continued interior ice-sheet growth, but that surface melting and accelerated flow increased thinning rates at the ice-sheet margins. Airborne topographic lidar data complement the spaceborne record, and observations made as part of NASA's Program for Arctic Regional Climate Assessment (PARCA) project over south-central Greenland (1993–99) indicate ice-sheet thickening at a rate of $0.05\text{--}0.10 \text{ m a}^{-1}$ west of the southern ice divide (Krabill and others, 2000). Interpretation of these satellite and airborne data for south-central Greenland can be improved by including in situ measurements made at three field sites first occupied by The Ohio State University (OSU) in 1980 and again in 1981. At each site, in situ surface elevation, ice thickness, surface velocity, surface gravity and firn physical property measurements were first

carried out by a team led by Ian Whillans (Whillans and others, 1984, 1987; Kostecka and Whillans, 1988). Whillans designated the sites as Dye 3, central cluster and western cluster (Fig. 1). Whillans's original data are summarized by Van der Veen and others (2000).

Subsequent to Whillans's study, in situ GPS surface measurements were repeated at several OSU sites as part of the PARCA surface traverse program (Thomas and others, 2000): three central cluster sites in 1993 and again in 1995. Several of the central and western sites were reoccupied during June 2003, 2004 and 2005, and surface gravity, position and elevation were remeasured by the author using GPS instruments and gravimeters. All of the original cluster sites have been overflown on an opportunity basis by the Wallops Flight Facility Airborne Topographic Mapper (ATM) (Krabill and others, 1995a; Thomas and others, 1999). The last overflight occurred in 2011 as part of NASA's Operation IceBridge, which is tasked with assuring continuity of the ice-sheet elevation change record during the period between ICESat and ICESat-2. In fact, ICESat data acquired in the vicinity of one benchmark in each cluster allow for an estimate of elevation change during the ICESat period of observations.

The combined results represent a 30 year time series of surface property change. It is one of the few accurate and long-term records of multiple ice-sheet surface properties on the interior Greenland ice sheet (e.g. Paterson and Reeh, 2001). This paper summarizes observations at the clusters and discusses possible scenarios to explain changing thickening rates and velocities across this portion of the ice sheet.

THE OSU CLUSTERS

Whillans and others (1984) made geodetic and other geophysical measurements at the cluster sites in 1980 and 1981 using Doppler satellite-tracking receivers tied to Doppler receiver base stations at fixed sites in Søndre

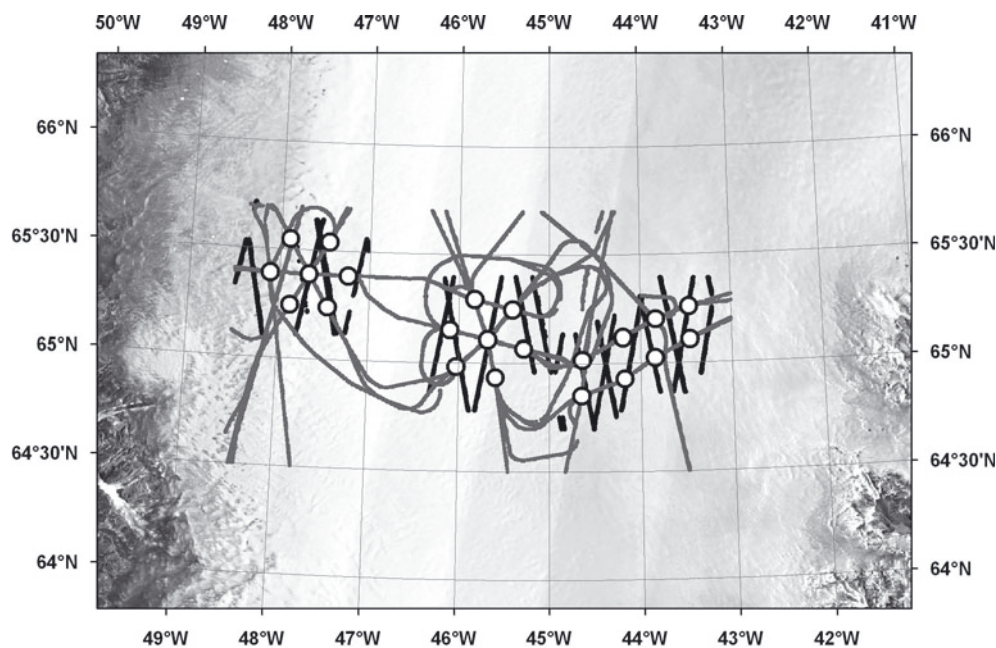


Fig. 1. Locations of original OSU cluster nodes (circles), ATM overflights (gray) and ICESat observations (black). The western cluster ($\sim 47.5^\circ$ W) and central cluster (45.6° W) are located on the western side of the ice divide, which in turn is located at the western extent of the Dye 3 cluster. The central node for the two hexagonal clusters is labeled 01. The due east node becomes 02, with the labels increasing in a clockwise direction. At Dye 3, the most northeasterly site is labeled 01, progressing up and down till station 08 in the southwest corner. A two-digit prefix is appended to each node to identify the cluster (e.g. 1001 is the central node at the western cluster; 2001 is the central node at the central cluster; 3001 is the most northeasterly node at the Dye 3 cluster). Background is a RADARSAT-1 synthetic aperture radar (SAR) image mosaic.

Strømfjord and Nuuk on the west coast of Greenland. Receivers were positioned at the node points shown in Figure 1. Sites were marked with accumulation rate poles, usually visible for 1–2 years after initial emplacement. Barometric measurements of relative ice elevation were used to interpolate elevations between the nodes.

Sites were subsequently resurveyed using Whillans's geographic coordinates as benchmarks. GPS receivers, operated on the surface and tied to a base station in Søndre Strømfjord, were used to relocate the sites and this was successfully done to within ~ 20 m based on the post-processing results. Receivers were deployed usually in early June and for several hours to several days to determine the precise locations where a new aluminum pole was deployed. GPS data reduction was carried out by the Wallops Flight Facility team (personal communications from J. Sonntag, 2003–06). Repeated measurements were used for estimating surface displacement and accumulation. Aircraft laser altimeter flights were also designed to resurvey the sites (Krabill and others, 1995a; Thomas and others 1999). The most recent of these missions was part of the Arctic 2011 Operation IceBridge campaign. Because the cross-track scan of the ATM is ~ 200 m when the aircraft is flown 500 m above the ice-sheet surface, elevation data were typically collected within a few meters of the designated measurement site.

Gravity measurements were made at all the sites in 1981 (Jezek and others, 1985) and at the central site in 2003 using a Lacoste Romberg meter. Data were referenced to the International Gravity Station Network by occupying several stations in and around Søndre Strømfjord and are estimated to be accurate to ~ 0.02 mgal. The meter was transported to the sites via surface vehicle in 1981 and via a Twin Otter aircraft in 2003. The gravity measurements were made within ~ 1 m of the GPS antenna in the field.

ICESat data are distributed across the cluster sites. However, only three sites were located close enough to ICESat tracks to enable a reasonably accurate slope correction. The near-coincident sites were: western cluster 1001, which is the center node of the rosette; central cluster 2001, which is also the central node; and 3001, which is the farthest northeast point in the Dye 3 cluster.

PROCESSING

Processing began by transforming all surface elevation data to the International Terrestrial Reference Frame (ITRF) 2000 and the World Geodetic System 1984 ellipsoidal elevation (WGS84). Absolute gravity values were determined by drift-correcting the field measurements and tying the result to the local International Gravity Station Network sites.

Displacements between repeat in situ GPS measurements were computed along a spheroidal surface using the Vincenty formula. Measurements were generally straightforward at the central site where aluminum poles used to mark the measurement location stayed in place between years. Western cluster data were adjusted for the fact that poles were tilted by melt.

Individual laser-shot data acquired by the ATM instrument, termed q-fit by the ATM project (Krabill, 2009), were incorporated into the elevation records for each OSU station. As noted above, shot locations did not coincide exactly with the OSU stations. Consequently, several shots about the station were interpolated to the station position.

ICESat observations are displaced from the cluster nodes. Similarly, sites reoccupied with GPS instruments were typically displaced from the intended site by several tens of meters. Hence, in order to extrapolate the elevation and other measurements to the intended location, slope

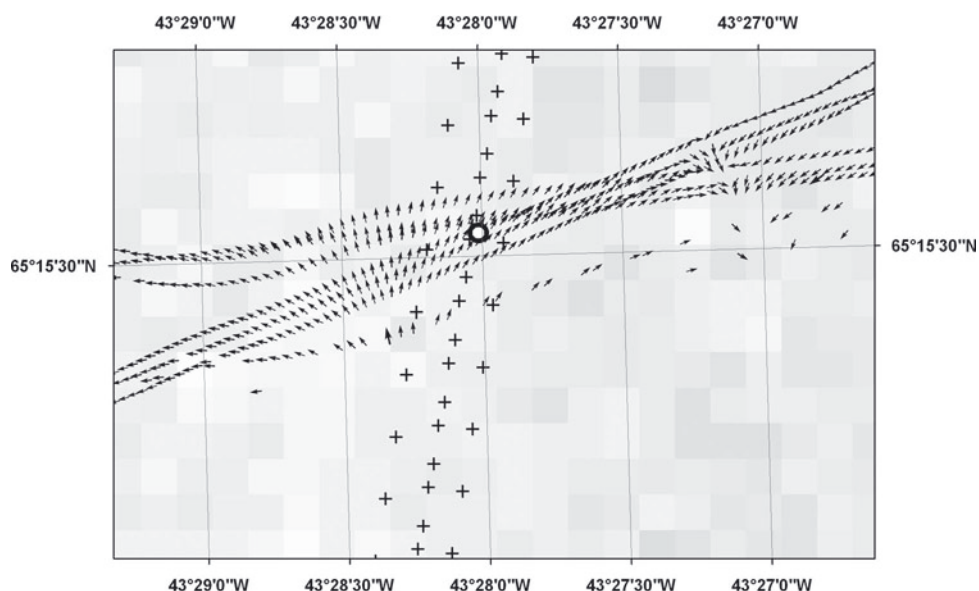


Fig. 2. Local variations in surface slope (arrows) located near the Dye 3 cluster 3001 data point (circle). ICESat data are shown by crosses. There is a local rotation of the slope vectors in the vicinity of the cluster point. Accounting for the local rotation is important for properly slope-correcting the ICESat data to the cluster point.

corrections were applied by computing the local average slope vector and computing the scalar product of the slope and measurement-offset vectors. Average slopes can be deduced from the elevation contour maps constructed from the original OSU data. Regional slope at the lower cluster station 1001 is ~ 0.01 . Slopes are slightly less at Central (~ 0.004) and Dye 3 (~ 0.007). These tend to mask small-scale changes in slope that can be important in local corrections. Consequently, slopes provided as part of the ATM ICESSEN 1 km product were used to refine slope estimates (Fig. 2; Krabill, 2010). The advantage of using the ATM data, which regionally are consistent with the digital elevation model (DEM)-derived slopes, is shown in Figure 2 for the 3001 benchmark in the Dye 3 network. Slope magnitude is locally high (0.015) and there is a rotation of the slope vector in the vicinity of the cluster node. The rotation is documented by several observations made in different years and may represent either a flow feature or could be an anomaly associated with the now abandoned Dye 3 radar station. In any case, the local correction is key to making a proper comparison between the ICESat and in situ data at this site.

After all corrections, estimated accuracies for the elevation datasets are: 20 cm uncertainty in ICESat data largely due to slope correction uncertainties; 10–20 cm uncertainties in ATM data (Krabill and others, 1995b); 5 cm uncertainties for in situ slope-corrected GPS data (personal communication from J. Sonntag, 2011); and 10–20 cm uncertainties in Doppler satellite elevations (Bolzan, 1994; Van der Veen and others, 2000).

ELEVATION CHANGE IN SOUTH-CENTRAL GREENLAND

The time series of in situ Doppler satellite and GPS elevations, ATM airborne lidar measurements and ICESat data for the OSU stations are shown in Figures 3–5. ICESat data are the average for all observations in a particular year, which on the one hand introduces a seasonal bias because

of limited sampling but on the other hand tends to reduce random errors. Remaining biases between ICESat data and the other data can be attributed to a small error in average slope. ICESat trends are generally consistent with the other observations. Both airborne and in situ observations were made at the central cluster stations 2001, 2005 and 2006 in 1993. Differences are on the order of 10–20 cm, so averaged values are used here.

From 1980 to 2005 most stations west of the ice divide convincingly show increasing surface elevation. The average thickening rate is $0.10 \pm 0.2 \text{ m a}^{-1}$ at the western cluster through 2005, which is somewhat less than the 0.16 m a^{-1} that Davis and others (2000) report and also the $0.142 \pm 0.04 \text{ m a}^{-1}$ thickening reported by Thomas and others (1999) based on data from 1980–93/94. More careful inspection of the western cluster data indicates that thickening slowed from 1995 to ~ 2006 and then gave way to thinning, which is consistent with the observations of Zwally and others (2011) using ICESat data alone. Thinning began sometime between 1998 and 2004 at the westernmost sites (1004, 1005 and 1006), which even in 1980 were characterized by significant surface melt. By 2011, most of the western cluster nodes thinned by almost 1 m from the earlier peak elevations.

Elevation change is more uniform across the central cluster. Thomas and others (1999) found that the ice thickened by $0.094 \pm 0.04 \text{ m a}^{-1}$ through 1993/94. Through 2005, the average thickening rate is slightly less, $0.08 \pm 0.02 \text{ m a}^{-1}$. There are again weak indications for changes in the thickening rate between 1995 and 1998 probably due to short-term fluctuations in accumulation rate. Thickening rates change between 2005 and 2006, initiating a period of negligible elevation change and perhaps thinning, an observation which so far seems absent in other studies (e.g. Zwally and others, 2011).

Elevation changes at the Dye 3 cluster are well correlated with position relative to the ice divide and are consistent with comparisons between ICESat and ERS/ATM data (Zwally and others, 2011). Using earlier ATM data, Thomas and others

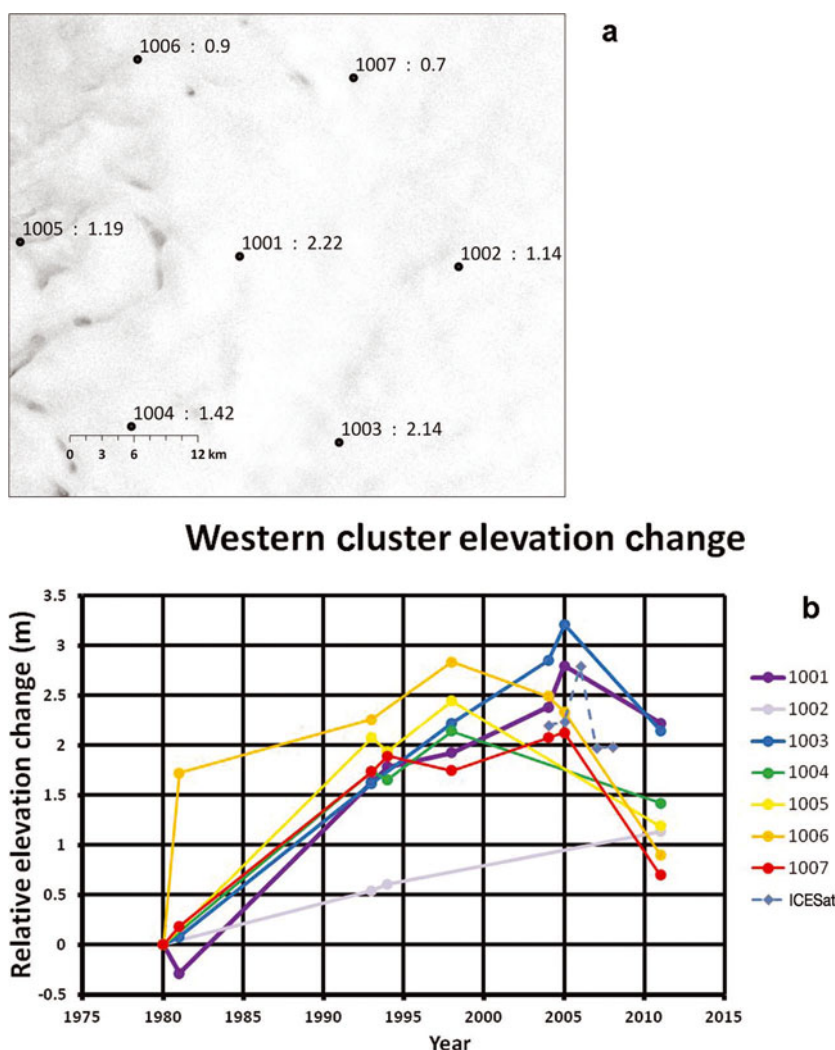


Fig. 3. (a) Station locations mapped onto a RADARSAT SAR image. The station number (left) is separated by a colon from the total change in elevation (m) between 1980 and 2011. Small surface lakes are evident as irregular dark patches near stations 1005 and 1006. (b) Combined in situ Doppler satellite and GPS data along with ATM lidar observations. Elevations are relative to the 1980 elevation at each station. Measurements in a particular year are averaged. Geographically interpolated ICESat data relative to station 1001 are shown in the later part of the record.

(1999) estimated thinning rates for OSU stations closest to the divide to be $0.01 \pm 0.04 \text{ m a}^{-1}$ and for stations furthest from the divide to be about $0.09 \pm 0.04 \text{ m a}^{-1}$ (1980–93/94). Continuing the record through 2011, the ice sheet is thinning at a rate of $\sim 0.11 \pm 0.02 \text{ m a}^{-1}$ at stations 3001 and 3002 east of the divide. Nearer the divide at station 3005, thinning rates drop to about $0.03 \pm 0.02 \text{ m a}^{-1}$. Elevation at station 3008, which is very nearly at the 2011 position of the ice divide, increased $\sim 0.05 \pm 0.02 \text{ m a}^{-1}$ over the observation period. The next two westerly stations (3006 and 3007) began to thicken sometime between 1998 and 2011.

In addition to data purposely collected at each cluster node, there are two ATM flights (1994 and 2011) which very nearly repeat across the three OSU clusters. Figure 6 shows the location of the cluster sites, the position of the overlapping flight-lines, and flowlines derived from geoidal surface slopes (DEM provided by B. Csatho). Figure 6 also shows the large-scale cross-sectional topography of the ice sheet based on the ICESat data product. ICESat data were selected here because surface slopes in the vicinity of the ice divide are small and data averaging reduces random errors due to sastrugi and other small-scale topography.

Discrepancies between the 1994 and 2011 elevation data notable at this scale are attributable to horizontal deviations between the trajectories of each flight. Two groups of 1994 low-elevation results are taken to be noise.

Figure 7 shows the aircraft ground tracks crossing the ice divide, along with an enlargement of the surface elevations at the divide. Again elevation differences west of -44.7° are attributable to ground track shifts. However, between -44.7° and -44.5° , the observations almost completely overlap. Notice that the position of the ice divide is more clearly defined in 2011 whereas there seems to be a relative depression near the divide in 1994 (between -44.64° and -44.66°). The depression may be exaggerated by small turns in the aircraft trajectory over this location. Also note that the ice divide thickened by $>1 \text{ m}$ during this period. On average, there seems to be little evidence that the ice divide has migrated, which contradicts the conclusion of Whillans and others (1987) who invoked divide migration to explain uncorrelated surface slope vectors and velocity vectors. The discrepancies between these two vector fields may be more reasonably reconciled by the apparently short-term changes in local ice-divide small-scale topography.

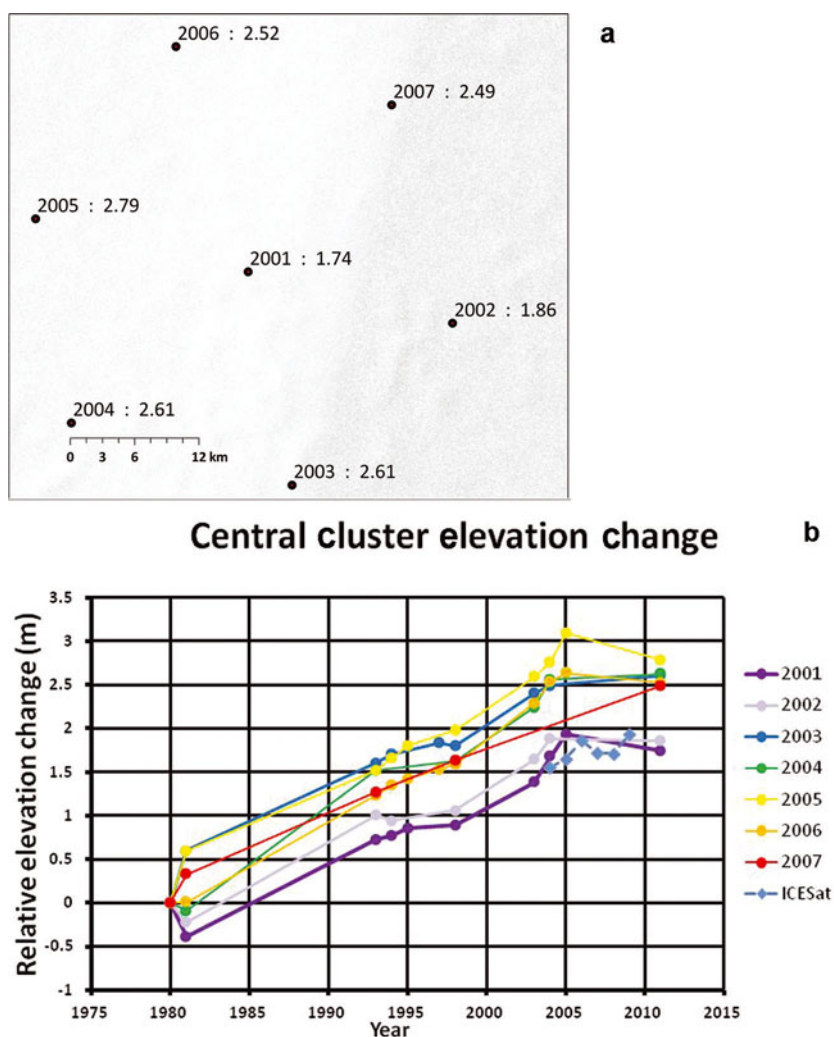


Fig. 4. (a) Station locations mapped onto a RADARSAT SAR image. The station number (left) is separated by a colon from the total change in elevation (m) between 1980 and 2011. (b) Combined in situ Doppler satellite and GPS data along with ATM lidar observations. Elevations are relative to the 1980 elevation at each station. Measurements in a particular year are averaged. Geographically interpolated ICESat data relative to station 2001 are shown in the later part of the record.

IN SITU SURFACE GRAVITY, VELOCITY AND ACCUMULATION RATE MEASUREMENTS

Gravity, surface horizontal displacement and accumulation data were collected in addition to the surface elevation data reviewed above. These additional datasets are useful for better interpreting the elevation trends as discussed below.

Gravity data collected at the central cluster can be used as an independent check on the ice-sheet thickening rates. Measurements using relative gravimeters were converted to absolute gravity values using fiducials of the International Gravity Station Network. Neglecting mass changes, the elevation data can be interpreted in terms of the free-air gravity correction of $0.3086 \text{ mgal m}^{-1}$. Figure 8 shows the absolute gravity data less a constant value for display purposes. Gravitational acceleration decreases with time, consistent with surface elevation increasing at $\sim 0.06\text{--}0.07 \text{ m a}^{-1}$ for the observation period. This value is slightly less than the observed thickening rate but is within the estimated gravity equivalent error of $\sim 0.02 \text{ m a}^{-1}$. The gravity trend lends support to the consistency between the different elevation measurements and measurement methodologies used to compile the long-term elevation time series presented above.

Whillans measured surface velocity and accumulation rate at all of the cluster nodes using repeat Doppler satellite observations. In 1993 during the initial leg of a traverse about the 2000 m elevation contour of the ice sheet (Thomas and others, 2000), station 2006 was occupied. A revisit enabled the velocity to be estimated ($11.19 \pm 0.06 \text{ m a}^{-1}$, 299° azimuth; Van der Veen and others, 2000). Van der Veen and others (2000) compared this result with the earlier 1980/81 epoch data and found a slight increase of $0.24 \pm 0.15 \text{ m a}^{-1}$. They hesitated to conclude that there was a positive increase based on this single measurement, so velocity and accumulation measurements were repeated at the central cluster from 2003 to 2005. Surface velocities for the central cluster are shown in Figure 9. Van der Veen and others (2000) estimate the speed accuracy from Doppler satellite data to be $\sim 10\text{--}20 \text{ cm a}^{-1}$. In cases where GPS data are used to estimate speeds, we estimate the errors to be $< 10 \text{ cm a}^{-1}$ and largely attributable to slight tilts in the survey poles. Velocities increase by $\sim 0.5\text{--}0.7 \text{ m a}^{-1}$ over the observation period, though there is weak evidence for a decrease in the later 2 years.

As part of the PARCA program (Thomas and others, 2000), three velocity measurements were made within 5–20 km of the original OSU lower cluster sites in 1996/97 (Van der

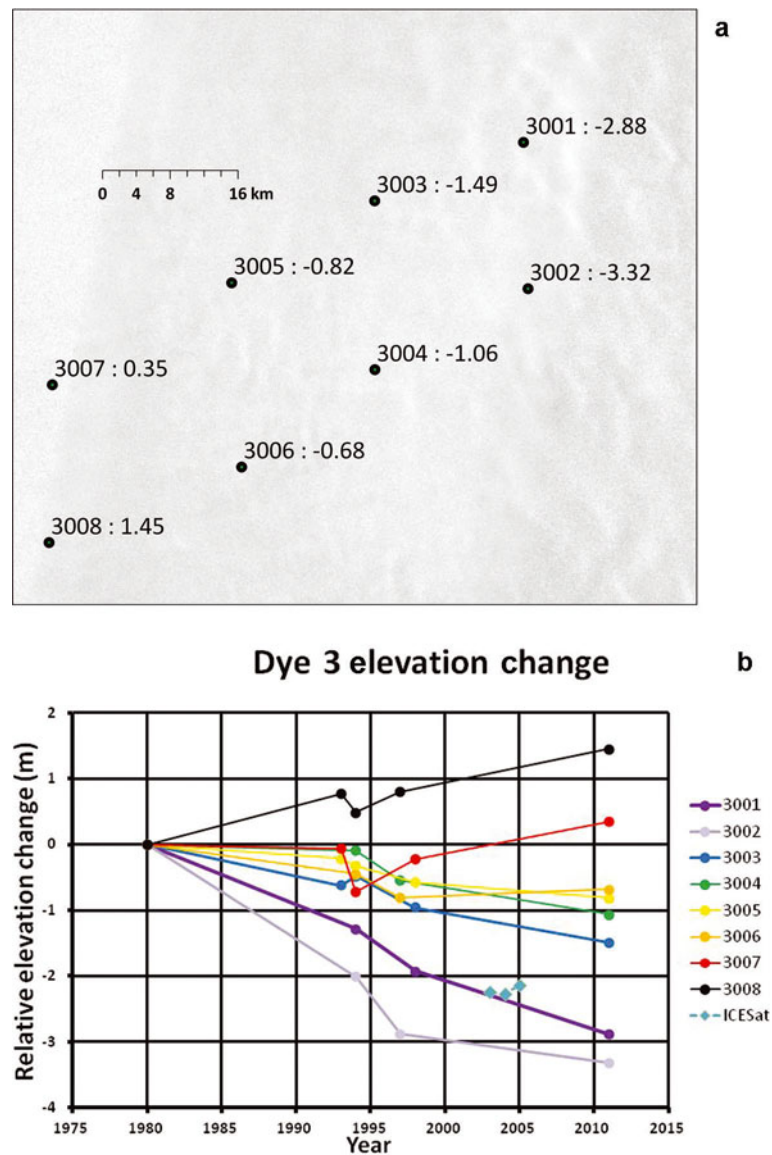


Fig. 5. (a) Station locations mapped onto a RADARSAT SAR image. The station number (left) is separated by a colon from the total change in elevation (m) between 1980 and 2011. (b) Combined in situ Doppler satellite and GPS data along with ATM lidar observations. Elevations are relative to the 1980 elevation at each station. Measurements in a particular year are averaged. Geographically interpolated ICESat data relative to station 3001 are shown in the later part of the record.

Veen and others, 2000, fig. 31). Because of the spatial displacement between observation sites, Van der Veen and others (2000) suggested that velocities had not changed over the 15 year period or at best the changes were small. Table 1 lists velocities for the 2003/04 and 1980/81 intervals at the western cluster. As noted, the aluminum marker poles at all

of these locations tilted during the 2003/04 season and so a correction based on the tilt was applied. Speed errors are estimated to be $\sim 1 \text{ m a}^{-1}$ because of the uncertainty in the tilt correction, so no trend lines are inferred. However there is a weak suggestion that speeds increased at two of the stations (1003 and 1006).

Table 1. Western cluster velocity

Station	2004/05		1980/81		2004–1980	
	Speed m a^{-1}	Azimuth $^{\circ}$	Speed m a^{-1}	Azimuth $^{\circ}$	Δ speed m a^{-1}	Δ azimuth $^{\circ}$
1001	35.70	288	35.76	288	-0.06	0
1003	36.83	290	36.07	290	0.76	0
1006	44.63	284	44.05	285	0.59	-1

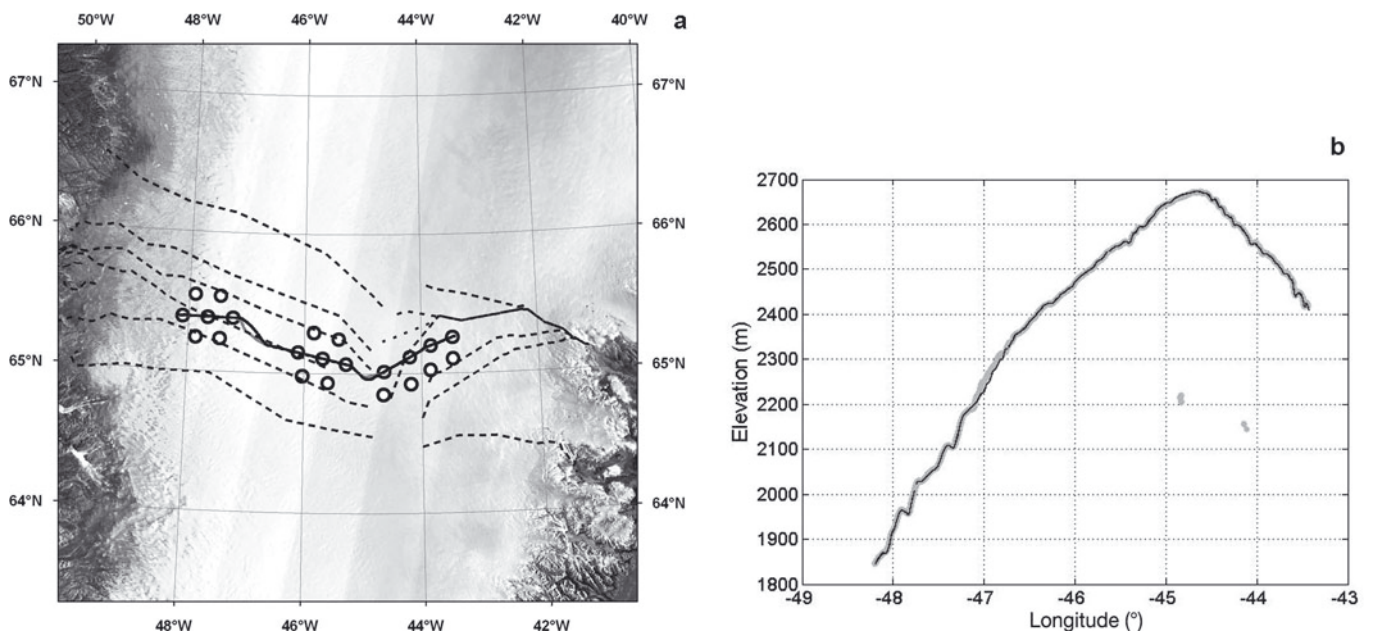


Fig. 6. (a) Flowlines (dashed black) derived from a high-resolution DEM (provided by B. Csatho). White circles are cluster nodes. The bold black line connecting the cluster stations is the 2011 ATM near-repeat ground track, and the barely visible gray line beneath the black line is the corresponding track flown in 1994. (b) ICESat surface elevation along the near-repeat tracks (thin black: 2011; thick gray: 1994). Elevation discrepancies of 10–20 m and observable on the graph at this scale are attributable to differences in aircraft trajectories. Two groups of unreasonably low elevation data (10–20 data points, each falling at ~2150 m elevation) recorded in 1994 are dismissed as noise.

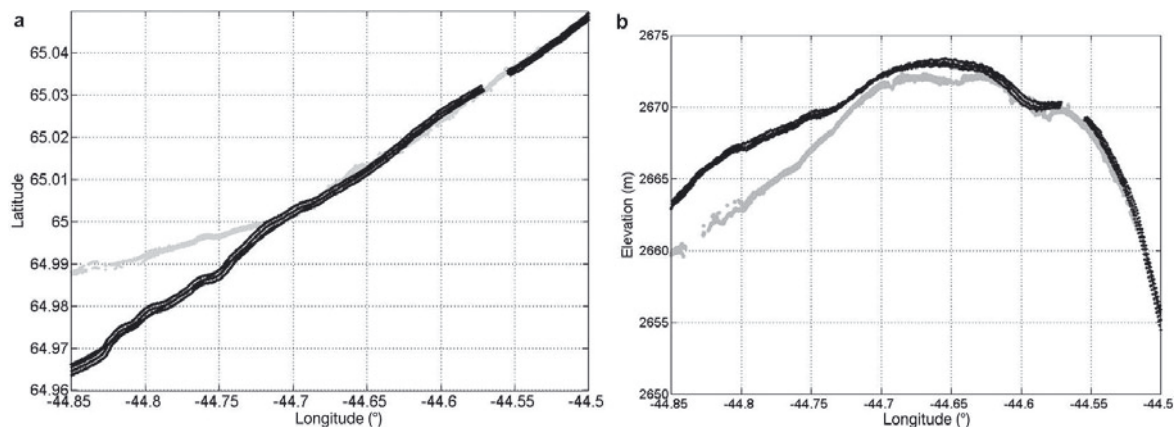


Fig. 7. (a) Enlargement of 1994 (gray) and 2011 (black) surface tracks. The three cross-track observations are fitted elevations provided with the ATM ICESat product. (b) Surface elevation across the ice divide. The 1994 and 2011 measurements between -44.66° and -44.65° are offset by ~ 100 m north/south, else there is geographical overlap between -44.72° and -44.05° . In the overlap region the data represent meaningful elevation change estimates. The longitude of station 3007 is -44.64° .

Accumulation was estimated at several central cluster sites by remeasuring aluminum pole heights above the surface. Pole height changes were converted to annual water equivalent using near-surface pit density data. The firn-core-derived results from Whillans and others (1987) and later revised by Van der Veen and others (2001) along with the results from 2003 and 2004 are shown in Table 2. Averaged over the ice sheet, interannual variability of accumulation rate is $>6 \text{ cm w.e. a}^{-1}$ and higher still in the south (Burgess and others, 2010), so a trend cannot be strictly inferred from this limited sampling. Note only that the later observations are $2\text{--}4 \text{ cm a}^{-1}$ higher than the earlier data.

Accumulation data were collected at the western and Dye 3 networks during the 1980 and 1981 campaigns.

Table 2. Central cluster accumulation rate (cm w.e. a^{-1})

	Accumulation		
	1980	2003	2004
2001	38.3	39.9	42.2
2002	36.1	43.0	
2003	40.7	41.0	
2004	37.2	46.5	
2005	36.9	39.9	42.6
2006	35.6	41.6	33.4
Average	37.47	41.99	39.40

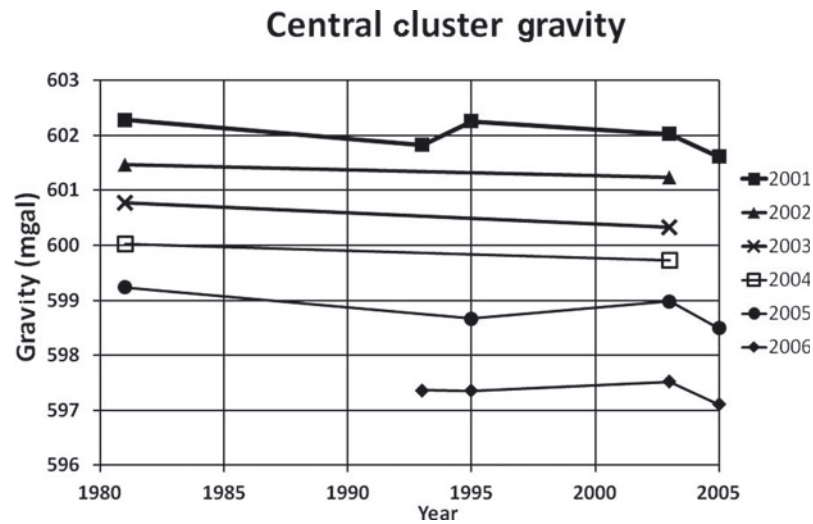


Fig. 8. Gravity data at the central cluster. The average decrease in gravity corresponds to a net elevation change of ~ 1.6 m over the 25 year period and based on a free-air anomaly correction with elevation of ~ 0.3086 mgal m^{-1} .

Average accumulation was 38.6 cm w.e. a^{-1} at the western cluster and 43.1 cm w.e. a^{-1} at three sites that straddle the divide at Dye 3 (Van der Veen and others, 2001). These spatial accumulation rate patterns are similar to those modeled by Cullather and Bosilovich (2011, fig. 7).

DISCUSSION

The OSU network traverses two different glacial regimes. West of the ice divide, ice flows approximately northwest towards its termination on the ice-free land. East of the ice divide, ice channels into an outlet glacier that drains into Pikiutdleq Bay (Fig. 6) where coastal glaciers are known to be thinning.

Stations west of the ice divide

Here the ice sheet above 1800 m thickened at least up till 2005. This is attributable to net mass gain as suggested by Kosticka and Whillans (1988), who found a positive balance of 0.06 ± 0.08 m a^{-1} for the average thickening in the vicinity

of the OSU measurements west of the ice divide, and also by Thomas and others (2000) who found thickening of ~ 0.066 m a^{-1} . Similarities between the two flux-estimated thickness trends and those reported here (0.10 and 0.08 ± 0.02 m a^{-1} for western and central clusters, respectively) indicate that the surface data are dominated by net changes in total mass rather than short-term interannual fluctuations in firn column density, at least for the period prior to about 2005.

After about 1998, there is a gradual, eastward-trending, thinning signature with time at the western cluster. This is likely due to the fact that surface melt is steadily increasing across Greenland, which contributes to significant mass loss in southern Greenland (Zwally and others, 2011). Because most of southern Greenland experiences some period of melt, Bhattacharya (2010) analyzed melt onset, end and duration for sectors distributed about Greenland. His analysis of the sectors containing the OSU western and central cluster sites shows that melt duration nearly doubled from 1978 to 2005, though the increase was roughly linear (0.81 ± 0.17 melt days a^{-1}). Melt occurred over 100% of the

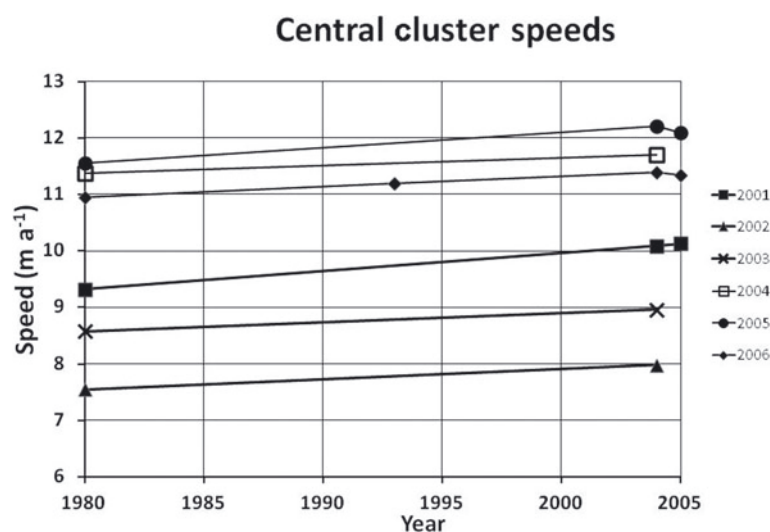


Fig. 9. Central cluster speeds from measurements of Doppler satellite and GPS station displacements. On average, surface speed increased at a rate of ~ 0.02 m a^{-1} .

study area between 1985 and 1991 and from 1997 till the end of his analysis in 2008. Even though this portion of the ice sheet terminates on a less dynamic landward margin, the consequence of increased melt is a net thinning of the ice sheet in the ablation zone. Wang and others (2012) address the question of how a thickness perturbation in the ablation zone will influence the behavior of the ice sheet upstream. They find that thinning propagates upstream over time-spans on the order of a decade. Consequently, it is tempting to speculate that the thinning progression observed at the western cluster and the change in thickening rate at the central cluster are attributable to a thickness perturbation propagating inland from the ablation zone. Although the data presented here preclude a definitive conclusion on that point, the model predictions and observations to date are consistent and argue for the importance of continued measurements across the ice sheet as well as around the more dynamic margins.

Coincident with thickening at the central cluster, the surface velocity increased. An increase in velocity results from an increase in the driving stress or a decrease in other resistive stresses. For an ice sheet frozen to the bed, the driving stress is related to the surface slope. The available data enable us to investigate whether the measured velocity increases in the central cluster are consistent with changes in the driving stress. Assuming laminar flow and a frozen bed, the surface velocity U_s is given by

$$U_s = \frac{2A}{(n+1)} (\rho g)^3 H^4 \left(\frac{\partial h}{\partial x}\right)^3 \quad (1)$$

where n is the flow law exponent taken to be 3, ρ is the density, g is the gravitational acceleration, H is the ice thickness and $\partial h/\partial x$ is the slope.

The variation in slope for a given variation in velocity is

$$\frac{d\left(\frac{\partial h}{\partial x}\right)}{\partial U_s} = \frac{2dU_s}{3A(\rho g)^3 H^4 \left(\frac{\partial h}{\partial x}\right)^2} \quad (2)$$

Over the 25 year period the surface speed increases by no more than $\sim 1 \text{ m a}^{-1}$, and taking the local slope to be 0.006 the corresponding change in slope over 25 years is 0.0009–0.0002, depending on the choice of hardness parameter, A , selected here to be either 7×10^{-18} or $2 \times 10^{-18} \text{ Pa}^{-3} \text{ a}^{-1}$, depending on choice of an average temperature between -20°C and -25°C (Van der Veen, 1999, fig. 2.6, p.17). Now the change in slope along a length Δx of flow is

$$\Delta s = \frac{\Delta h_0 - \Delta h_i}{\Delta x} \quad (3)$$

where Δh_0 is the change in elevation at the downstream end of the flowline and Δh_i is the change at the upstream end. Stations 2002 and 2005 are roughly situated along the flowline and $\sim 40 \text{ km}$ apart. For the change in slope noted above, the difference between the changes in output and input elevation should be between 36 and 10 m, again depending on our choice of A . The difference from Figure 4 is at most 0.5 m, which in this case actually flattens the ice sheet, as confirmed by direct inspection of the 1994–2011 repeat flight described in Figure 6, which also shows negligible slope change and implies negligible change in driving stress.

The central cluster is located far from important shearing margins, arguing against a change in lateral drag. Similarly, it seems unlikely that a change in basal drag through increased

basal melting is responsible for the velocity increase in regions where ice thicknesses approach 2000 m. Left are changes in longitudinal stress which seem to be the most plausible agent given the dramatic changes occurring about all of coastal Greenland (Wang and others, 2012).

Given the increase in velocity west of the divide, one might expect ice-sheet thinning to result from increased longitudinal flux. Yet thickening seems to coincide with velocity increase. To investigate this observation, consider the contribution of long-term increasing accumulation rate to the increasing velocity. Written in terms of flux gates, the continuity equation for each observation epoch is

$$\left(\frac{dh}{dt}\right)^{\text{year}} = -\left(\frac{w_0 H_0 V_0 - w_i H_i V_i}{\text{Area}}\right)^{\text{year}} + (\dot{a})^{\text{year}} \quad (4)$$

The thickening rate at the central cluster was roughly constant over the period of the 1980–2005 observations, i.e. the time rate of thickness change is negligible so we can then relate time rates of velocity change to time rates of accumulation change. We do this by separately writing Eqn (4) using the parameters for each epoch, differencing the resulting two equations and setting the difference to zero. To get an analytic expression for determining the equivalent speed change for a given accumulation rate change, specify a flowband of width w_1 at the ice divide to the central cluster where the flowband width is w_2 . Approximate the flowband by an isosceles trapezoid to get a rough analytic estimate of area. Assume uniform accumulation rates over the entire study area. Further assume the position of the ice divide has remained fixed and the velocity at the ice divide is close to zero. This leads to a rough estimate for the change in speed (sp) with a change in accumulation rate at the central cluster:

$$\Delta \text{sp} = \Delta \dot{a} \frac{L}{2H} \left(1 + \frac{w_1}{w_2}\right) \quad (5)$$

where L is the distance from the central cluster ($\sim 47 \text{ km}$) to the ice divide, H is the thickness at the central cluster ($\sim 1900 \text{ m}$) and the ratio of the flowband widths is ~ 0.7 (Fig. 6). Taking the total change in accumulation rate over the 25 year period to be $\sim 0.04 \text{ m a}^{-1}$ from the limited in situ accumulation data, but which is consistent with the 1958–2007 surface mass-balance trend presented by Ettema and others (2009) but smaller in magnitude, the total change in speed is $\sim 0.8 \text{ m a}^{-1}$ over the same period. This is slightly faster than observed, but given the simplifying assumptions, the estimate plausibly argues that long-term accumulation rate increases sufficiently to compensate the ice thickness for the increase in ice speed.

Stations east of the divide

Turning to the sites near Dye 3, up until the most recent observations the ice thinned (-0.01 to $-0.11 \pm 0.02 \text{ m a}^{-1}$ excluding station 3008) in a pattern well correlated with distance from the divide and consistent with satellite observations (Zwally and others, 2011). At the divide, thickness has steadily increased over the observation period ($0.05 \pm 0.02 \text{ m a}^{-1}$). Using a flux-based approach for a larger area encompassing the Dye 3 cluster, Thomas and others (2000) report thinning rates between -0.108 and -0.295 m a^{-1} . Ettema and others (2009) find negative surface mass-balance trends from nearly the ice divide to the southeast coast from 1958 to 2007. The combined observations again suggest a net mass loss associated with the thinning away from the divide. Thinning trends become

more pronounced with distance from the divide, which is consistent with the negative surface balance trends reported by Ettema and others (2009). Also, the Dye 3 cluster ultimately feeds into a coastal outlet glacier where dramatic drawdown is occurring (Howat and Eddy, 2011). Increasing thinning rates with distance from the divide show that slopes are increasing, probably also in response to coastal draw-down. In the absence of a compensating increase in accumulation, this leads to a prediction of increasing velocities and velocity gradients away from the divide. This is confirmed by the velocity increases for coastal glaciers discharging into Pikiutdleq Bay as measured by Joughin and others (2010) for the period 2000/01–2005/06. The slow-down in thinning rates after 2005, as reported here, suggests the velocity trend will likely reverse.

CONCLUSIONS

Through about 2005, the interior south-central Greenland ice sheet west of the ice divide thickened. Even as the ice sheet thickened, local velocities increased. Starting perhaps as early as 1998, the most westerly sites started to thin and elevations at the central cluster sites were negligibly changed. Western thinning is a likely consequence of increased melt in the ablation zone, which may result in the upstream propagation of a thickness perturbation as described by Wang and others (2012).

Thinning rates increased with eastward distance from the ice divide till about 2005. Thinning is partly driven by decreasing accumulation rate trends and dynamic processes at the coast. There is now indication for a slowdown in thinning rates at most stations east of the divide and thickening at two of the stations closest to the divide.

The simpler ice dynamics at the divide and in the interior ice sheet (e.g. negligible lateral shear) means that elevation measurements there can be less dense than at the coast, where spatially complex and often rapid elevation changes are occurring. Nevertheless, and complementary to the modeling results by Wang and others (2012), these results show that the Greenland ice sheet is changing from terminus to divide, and measurement strategies designed to predict future changes and to estimate volumetric changes across the ice sheet need to appropriately cover the entirety of the ice sheet.

ACKNOWLEDGEMENTS

F. Baumgartner began this research with the author in 2003. R. Jezek and K. Farness were field assistants in 2004 and 2005, respectively. The Wallops Flight Facility Airborne Topographic Team led by W. Krabill provided invaluable support over the years of observations. B. Smith provided the ICESat data used in this analysis. J. Bolzan and J. Zwally provided numerous helpful comments. More recent field-work and data compilations were supported by grants from NASA's Cryosphere Program. Data from 2011 were collected as part of NASA's Operation IceBridge project. The author's work in 1980/81 was supported by the Office of Polar Programs of the US National Science Foundation.

REFERENCES

Bhattacharya I (2010) Analysis of surface melting and snow accumulation over the Greenland Ice Sheet from spaceborne microwave sensors. (PhD thesis, The Ohio State University)

- Bolzan JF (1994) *Surface velocities in central Greenland from Doppler satellite data*. The Ohio State University, Columbus, OH (Byrd Polar Research Center Report 8)
- Brooks RL, Campbell WJ, Ramseier RO, Stanley HR and Zwally HJ (1978) Ice sheet topography by satellite altimetry. *Nature*, **274**(5671), 539–543
- Burgess EW and 6 others (2010) A spatially calibrated model of annual accumulation rate on the Greenland Ice Sheet (1958–2007). *J. Geophys. Res.*, **115**(F2), F02004 (doi: 10.1029/2009JF001293)
- Cullather RI and Bosilovich MG (2011) The moisture budget of the polar atmosphere in MERRA. *J. Climate*, **24**(11), 2861–2879 (doi: 10.1175/2010JCLI4090.1)
- Davis CH, Kluever CA, Haines BJ, Perez C and Yoon YT (2000) Improved elevation-change measurement of the southern Greenland ice sheet from satellite radar altimetry. *IEEE Trans. Geosci. Remote Sens.*, **38**(3), 1367–1378 (doi: 10.1109/36.843031)
- Ettema J and 6 others (2009) Higher surface mass balance of the Greenland ice sheet revealed by high-resolution climate modeling. *Geophys. Res. Lett.*, **36**(12), L12501 (doi: 10.1029/2009GL038110)
- Howat IM and Eddy A (2011) Multi-decadal retreat of Greenland's marine-terminating glaciers. *J. Glaciol.*, **57**(203), 389–396 (doi: 10.3189/002214311796905631)
- Jezek KC, Roeloffs EA and Greishchar L (1985) A geophysical survey of subglacial geology around the deep-drilling site at DYE-3, Greenland. In Langway CC, Jr, Oeschger H and Dansgaard W eds, *Greenland ice core: geophysics, geochemistry and the environment*. American Geophysical Union, Washington, DC, 105–110 (Geophysical Monograph 33)
- Johannessen OM, Khvorostovsky K, Miles MW and Bobylev LP (2005) Recent ice-sheet growth in the interior of Greenland. *Science*, **310**(5750), 1013–1016 (doi: 10.1126/science.1115356)
- Joughin I, Smith BE, Howat IM, Scambos T and Moon T (2010) Greenland flow variability from ice-sheet-wide velocity mapping. *J. Glaciol.*, **56**(197), 415–430 (doi: 10.3189/002214310792447734)
- Kostecka JM and Whillans IM (1988) Mass balance along two transects of the west side of the Greenland ice sheet. *J. Glaciol.*, **34**(116), 31–39
- Krabill WB (2009) *IceBridge ATM L1B Qfit elevation and return strength*. NASA Distributed Active Archive Center, National Snow and Ice Data Center, Boulder, CO. Digital media: <http://nsidc.org/data/ilatm1b.html>
- Krabill WB (2010) *IceBridge ATM L2 Icessn elevation, slope, and roughness*. NASA Distributed Active Archive Center, National Snow and Ice Data Center, Boulder, CO. Digital media: <http://nsidc.org/data/ilatm2.html> (7 November 2009)
- Krabill W, Thomas R, Jezek K, Kuivinen K and Manizade S (1995a) Greenland ice sheet thickness changes measured by laser altimetry. *Geophys. Res. Lett.*, **22**(17), 2341–2344 (doi: 10.1029/95GL02069)
- Krabill WB, Thomas RH, Martin CF, Swift RN and Frederick EB (1995b) Accuracy of airborne laser altimetry over the Greenland ice sheet. *Int. J. Remote Sens.*, **16**(7), 1211–1222 (doi: 10.1080/01431169508954472)
- Krabill WB and 9 others (2000) Greenland ice sheet: high-elevation balance and peripheral thinning. *Science*, **289**(5478), 428–430 (doi: 10.1126/science.289.5478.428)
- Paterson WSB and Reeh N (2001) Thinning of the ice sheet in northwest Greenland over the past forty years. *Nature*, **414**(6859), 60–62 (doi: 10.1038/35102044)
- Thomas R and 6 others (1999) Greenland ice sheet elevation change since 1978 from radar and laser altimetry. *Polar Geogr.*, **23**(3), 169–184 (doi: 10.1080/10889379909377674)
- Thomas R and 6 others (2000) Mass balance of the Greenland ice sheet at high elevations. *Science*, **289**(5478), 426–428 (doi: 10.1126/science.289.5478.426)

- Van der Veen CJ (1999) *Fundamentals of glacier dynamics*. AA Balkema, Rotterdam
- Van der Veen CJ, Jezek KC, Mosley-Thompson E, Whillans IM and Bolzan JF (2000) Two decades of glaciological investigations in South and Central Greenland. *Polar Geogr.*, **24**(4), 259–349 (doi: 10.1080/10889370009377700)
- Van der Veen CJ, Mosley-Thompson E, Jezek KC, Whillans IM and Bolzan JF (2001) Accumulation rates in South and Central Greenland. *Polar Geogr.*, **25**(2), 79–162 (doi: 10.1080/10889370109377709)
- Wang W, Li J and Zwally HJ (2012) Dynamic inland propagation of thinning due to ice loss at the margins of the Greenland ice sheet. *J. Glaciol.*, **58**(210), 734–740 (doi: 10.3189/2012JoG11J187)
- Whillans IM, Jezek KC, Drew AR and Gundestrup N (1984) Ice flow leading to the deep core hole at Dye 3, Greenland. *Ann. Glaciol.*, **5**, 185–190
- Whillans IM and 6 others (1987) *Glaciologic transect in southern Greenland: 1980 and 1981 GISP-I data*. The Ohio State University, Columbus, OH (Byrd Polar Research Center Report 2)
- Zwally HJ, Brenner AC, Major JA, Bindshadler RA and Marsh JG (1989) Growth of Greenland ice sheet: measurement. *Science*, **246**(4937), 1587–1589 (doi: 10.1126/science.246.4937.1587)
- Zwally HJ and 11 others (2011) Greenland ice sheet mass balance: distribution of increased mass loss with climate warming; 2003–07 versus 1992–2002. *J. Glaciol.*, **57**(201), 88–102 (doi: 10.3189/002214311795306682)

MS received 9 February 2012 and accepted in revised form 30 August 2012